NATIONAL ADVISORY COMMITTEE FOR AERONAUTICS

TECHNICAL NOTE

No. 1443

SHEAR LAG IN A PLYWOOD SHEET-STRINGER COMBINATION USED FOR THE CHORD MEMBER OF A BOX BEAM

By Palamede Borsari and Ai-ting Yu

Massachusetts Institute of Technology

Washington

March 1948

NATIONAL ADVISORY COMMITTEE FOR AERONAUTICS

TECHNICAL NOTE NO. 1443

SHEAR LAG IN A PLYWOOD SHEET-STRINGER COMBINATION USED FOR THE CHORD MEMBER OF A BOX BEAM

By Palamede Borsari and Ai-ting Yu

SUMMARY

Theoretical and experimental investigations were made of the distribution of strains in a plywood sheet-stringer combination used as the chord member of a box beam acted upon by bending loads. The theoretical solution was obtained with the help of the principle of minimum potential energy and certain simplifying assumptions. Strain measurements were made on a built-up box beam by means of electrical-resistance strain gages connected with strain indicators. A very satisfactory agreement between the theoretical and experimental strains was obtained.

INTRODUCTION

The development of monocoque and semimonocoque structures in airplanes has introduced the shear-lag problem, which, in brief, results from the fact that box beams with thin, wide chord members do not follow elementary beam theory. The assumption of uniform normal stress distribution on fibers equidistant from the neutral axis of any transverse section is not justified for these beams. The deviation from uniform normal stress is caused by the shear deformation in the chord member of this type of structure, an effect not provided for in simple beam theory.

Various theoretical treatments have been carried out and numerous experiments have been conducted to check the adequacy of them, especially on isotropic or orthotropic metal structures. Very little information, however, is available on plywood construction. For plywood sheet-stringer combinations there appear to be no data.

The present investigation is a condensed version of a thesis presented to the Massachusetts Institute of Technology in partial fulfillment of the requirements for the degree of Master of Science in Aeronautical Engineering. The theoretical development presented in this thesis is due to Dr. Eric Reissner, who outlined to the authors the several steps necessary to obtain the solution.

SYMBOLS

x	spanwise rectangular coordinate measured from tip to root in midplane of cover sheet
y	transverse rectangular coordinate measured from longitudinal plane of symmetry to edge in midplane of cover sheet
z	coordinate axis perpendicular to neutral plane of beam measured from bottom to top cover
L	beam span
$2d$	beam width
h	beam depth
t	cover-sheet thickness
b	side-web width
A_{st}	area of cross section of nth stringer
E_x	modulus of elasticity of cover sheet in x-direction
E_{st}	modulus of elasticity of nth stringer
E_w	modulus of elasticity of side web
G_{xy}	modulus of rigidity of cover sheet referred to shearing stress acting parallel to x- and y-axes
u_{sheet}, v	displacements in midplane of cover sheet in x- and y-directions, respectively
u_{web}	displacement of side web in x-direction
w_{web}	displacement of side web in z-direction
M_x	applied bending moment
ϵ_x, γ_{xy}	strain components in cover sheet
ϵ_{st}	longitudinal strain in stringers
ϵ_{web}	longitudinal strain in side webs

DEVELOPMENT OF THEORY

By following the suggestions given by Reissner (reference 1), a complete solution of the shear-lag problem for the case of a sheet-stringer combination used as a chord member of a singly symmetrical box beam of constant cross section is presented. Further generalization of the method may be carried out with little difficulty, since the general procedure remains essentially the same for any common shape of beam or load.

Principle of Method

The method consists in expressing the total energy of the system as the sum of the energy of deformation (the volume integral of the strain-energy function) and the energy of external forces. Thus,

$$\pi = \pi_i + \pi_e \tag{1}$$

Following this, the differential equations of equilibrium are obtained from the theorem of minimum energy stated as: "The displacement which satisfies both the differential equations of equilibrium, as well as the conditions at the bounding surface, yields a smaller value for the potential energy of deformation than any other displacement, which satisfies the same conditions at the bounding surface" (reference 2). This can be written as

$$\delta\pi = 0 \tag{2}$$

Assumptions for Simplification of Problem

The expressions for π_i and π_e are based on the following simplifying assumptions:

(1) It is customary, in dealing with problems of this nature, to neglect the stretching ϵ_y of the sheet in the transverse direction, since it is very small as compared with the stretching in the spanwise direction. This assumption has been used even in "exact" analytical solutions, as shown in reference 3.

(2) Since $\epsilon_y = \frac{\partial v}{\partial y}$, if $\epsilon_y = 0$, v would be a function of x only. Here, however, we assume that the displacement

$$v = 0 \tag{3}$$

(3) Instead of assuming a parabolic distribution of stress as in reference 4, Reissner suggested a parabolic distribution of displacement of the sheet in the transverse direction. These displacements can be written in the form

$$u_{sheet} = u_0(x) + \left(1 - \frac{y^2}{d^2}\right) u_2(x) \tag{4}$$

(4) The linear side-web displacements are determined in such a way that cover-sheet and side-web normal displacements coincide along the line of junction, that is,

$$u_{web} = u_0(x) + u_1(x)\left(\frac{z}{h} - 1\right) \tag{5}$$

(5) The sheet is free from shear parallel to the z-axis. Such shear is carried by the webs only.

Equation (2) furnishes the differential equations for the determination of the unknown functions u_0, u_1, and u_2 of equations (4) and (5). Since

$$\epsilon_x = \frac{\partial u}{\partial x}$$

$$\epsilon_y = \frac{\partial v}{\partial y}$$

$$\gamma_{xy} = \frac{\partial u}{\partial y} + \frac{\partial v}{\partial x}$$

assumptions (1) and (2) are expressed by

$$\epsilon_y = \frac{\partial v}{\partial y} = 0$$

and

$$\frac{\partial v}{\partial x} = 0$$

Hence,

$$\left.\begin{aligned} \epsilon_x &= \frac{\partial u}{\partial x} \\ \gamma_{xy} &= \frac{\partial u}{\partial y} \end{aligned}\right\} \tag{6}$$

Then, since u_0, u_1, and u_2 are functions of x only, equations (3) and (4) imply a parabolic distribution of normal strains

$$\epsilon_{x_{sheet}} = \frac{\partial u}{\partial x} = \frac{du_0}{dx} + \left(1 - \frac{y^2}{d^2}\right)\frac{du_2}{dx} \tag{7}$$

and a linear distribution of shearing strain

$$\gamma_{xy} = \frac{\partial u}{\partial y} = -\frac{2y}{d^2}\, u_2(x) \tag{8}$$

along any transverse section.

Formulation of Problem

A cantilever box beam (or an equivalent simple beam having double the length of the cantilever span) is considered. The cross section is constant along the span and the beam is acted on by a given distribution of bending moment. The box beam is singly symmetrical. It has two side webs, with a sheet-stringer cover sheet on one side. (See figs. 1 and 2.) The centroids of all the stringers are assumed to be on the midline of the sheet; hence bending effect on the stringers is neglected.

The potential energy of the system is obtained from

$$\pi_{sheet} = \frac{1}{2}\int_0^L \int_{-d}^{d} t\left(E_x \epsilon_x^2 + G\gamma_{xy}^2\right) dx\, dy \tag{9}$$

$$\pi_{web} = \int_0^L \int_0^h bE_w \epsilon_w^2 \, dz \, dx \tag{10}$$

$$\pi_{st} = \sum_{n=1}^{K} \int_0^L A_{st} E_{st} \epsilon_{st}^2 \, dx \tag{11}$$

Neglecting the shear in the side webs yields

$$\gamma_{xz_{web}} = \frac{\partial u_{web}}{\partial z} + \frac{\partial w_{web}}{\partial x} = 0$$

$$\frac{\partial w_{web}}{\partial x} = -\frac{\partial u_{web}}{\partial z}$$

From equation (5),

$$\frac{\partial u_{web}}{\partial z} = \frac{1}{h} u_1(x)$$

Therefore,

$$\frac{\partial w_{web}}{\partial x} = -\frac{1}{h} u_1(x)$$

Again,

$$\pi_{load} = \int_0^L M_x \frac{d^2w}{dx^2} \, dx$$

Therefore,

$$\pi_{load} = -\int_0^L M_x \frac{du_1}{dx}\frac{1}{h}\,dx \tag{12}$$

Finally,

$$\pi = \frac{1}{2}\int_0^L \int_{-d}^{d} t\left(E_x\epsilon_x^2 + G\gamma_{xy}^2\right)\,dx\,dy + \int_0^L \int_0^h bE_w\epsilon_w^2\,dz\,dx$$

$$+ \sum_{n=1}^{K} \int_0^L A_{st}E_{st}\epsilon_{st}^2\,dx - \int_0^L M_x \frac{du_1}{dx}\frac{1}{h}\,dx \tag{13}$$

For minimum energy condition, from equation (2),

$$\delta\pi = \int_0^L \int_{-d}^{d} t\left(E_x\epsilon_x\delta\epsilon_x + G\gamma_{xy}\delta\gamma_{xy}\right)\,dy\,dx$$

$$+ \int_0^L \int_0^h 2bE_w\epsilon(x,w)\delta\epsilon(x,w)\,dz\,dx$$

$$+ \sum_{n=1}^{K} \int_0^L 2A_{st}E_{st}\epsilon_{st}\delta\epsilon_{st}\,dx$$

$$- \int_0^L M_x\,\delta\left(\frac{du_1}{dx}\right)\frac{1}{h}\,dx \tag{14}$$

From equations (6), (7), and (8), the variation of strains is given by

$$\delta\epsilon_{x_{sheet}} = \delta\left(\frac{\partial u_0}{\partial x}\right) + \left(1 - \frac{y^2}{d^2}\right)\delta\left(\frac{\partial u_2}{\partial x}\right)$$

$$\delta\gamma_{xy} = -\frac{2y}{d^2}\,\delta u_2$$

$$\delta\epsilon_{x_{web}} = \delta\left(\frac{\partial u_0}{\partial x}\right) + \left(\frac{z}{h} - 1\right)\delta\left(\frac{\partial u_1}{\partial x}\right)$$

Therefore,

$$\left(\epsilon_x \delta\epsilon_x\right)_{sheet} = \frac{\partial u_0}{\partial x}\,\partial\left(\frac{\delta u_0}{\partial x}\right) + \left(1 - \frac{y^2}{d^2}\right)\frac{\partial u_0}{\partial x}\,\partial\left(\frac{\delta u_2}{\partial x}\right)$$

$$+ \left(1 - \frac{y^2}{d^2}\right)\frac{\partial u_2}{\partial x}\,\partial\left(\frac{\delta u_0}{\partial x}\right) + \left(1 - \frac{y^2}{d^2}\right)^2\frac{\partial u_2}{\partial x}\,\partial\left(\frac{\delta u_2}{\partial x}\right)$$

$$\left(\epsilon_x \delta\epsilon_x\right)_{web} = \frac{\partial u_0}{\partial x}\,\partial\left(\frac{\delta u_0}{\partial x}\right) + \left(\frac{z}{h} - 1\right)\frac{\partial u_0}{\partial x}\,\partial\left(\frac{\delta u_1}{\partial x}\right)$$

$$+ \left(\frac{z}{h} - 1\right)\frac{\partial u_1}{\partial x}\,\partial\left(\frac{\delta u_0}{\partial x}\right) + \left(\frac{z}{h} - 1\right)^2\frac{\partial u_1}{\partial x}\,\partial\left(\frac{\delta u_1}{\partial x}\right)$$

Substituting these relations into equation (14) yields

$$\delta\pi = \int_0^L \int_{-d}^{d} \left\{ t\, E_x \left[\frac{\partial u_0}{\partial x} \partial\left(\frac{\delta u_0}{\partial x}\right) + \left(1 - \frac{y^2}{d^2}\right) \frac{\partial u_0}{\partial x} \partial\left(\frac{\delta u_2}{\partial x}\right) + \left(1 - \frac{y^2}{d^2}\right) \frac{\partial u_2}{\partial x} \partial\left(\frac{\delta u_0}{\partial x}\right) \right.\right.$$

$$\left.\left. + \left(1 - \frac{y^2}{d^2}\right)^2 \frac{\partial u_2}{\partial x} \partial\left(\frac{\delta u_2}{\partial x}\right) \right] + t\, G\, \frac{4y^2}{d^4}\, u_2 \delta u_2 \right\} dy\, dx$$

$$+ \int_0^L \int_0^h 2b\, E_w \left[\frac{\partial u_0}{\partial x} \partial\left(\frac{\delta u_0}{\partial x}\right) + \left(\frac{z}{h} - 1\right) \frac{\partial u_0}{\partial x} \partial\left(\frac{\delta u_1}{\partial x}\right) + \left(\frac{z}{h} - 1\right) \frac{\partial u_1}{\partial x} \partial\left(\frac{\delta u_0}{\partial x}\right) \right.$$

$$\left. + \left(\frac{z}{h} - 1\right)^2 \frac{\partial u_1}{\partial x} \partial\left(\frac{\delta u_1}{\partial x}\right) \right] dz\, dx$$

$$+ \sum_{n=1}^{K} \int_0^L 2\, A_{st}\, E_{st} \left[\frac{\partial u_0}{\partial x} \partial\left(\frac{\delta u_0}{\partial x}\right) + \left(1 - \frac{y_n^2}{d^2}\right) \frac{\partial u_0}{\partial x} \partial\left(\frac{\delta u_2}{\partial x}\right) + \left(1 - \frac{y_n^2}{d^2}\right) \frac{\partial u_2}{\partial x} \partial\left(\frac{\delta u_0}{\partial x}\right) \right.$$

$$\left. + \left(1 - \frac{y_n^2}{d^2}\right) \frac{\partial u_2}{\partial x} \partial\left(\frac{\delta u_2}{\partial x}\right) \right] dx - \int_0^L M_x \partial\left(\frac{\delta u_1}{\partial x}\right) \frac{1}{h}\, dx = 0$$

Integration with respect to y in the first integral and with respect to z in the second integral can now be carried out.

$$\int_{-d}^{d} dy = 2d$$

$$\int_{-d}^{d} \left(1 - \frac{y^2}{d^2}\right) dy = \frac{4}{3} d$$

$$\int_{-d}^{d} \left(1 - \frac{y^2}{d^2}\right)^2 dy = \frac{16}{15} d$$

$$\int_{0}^{h} dz = h$$

$$\int_{0}^{h} \left(\frac{z}{h} - 1\right) dz = -\frac{h}{2}$$

$$\int_{0}^{h} \left(\frac{z}{h} - 1\right)^2 dz = \frac{h}{3}$$

Substituting these values and grouping the terms accordingly, yields

$$\delta\pi = \int_0^L \left\{ \frac{\partial u_0}{\partial x} \partial\left(\frac{\delta u_0}{\partial x}\right)\left(t E_x d + b E_w h + \sum_1^n A_{st} E_{st}\right) \right.$$

$$+ \frac{\partial u_0}{\partial x} \partial\left(\frac{\delta u_2}{\partial x}\right)\left[\frac{2}{3} t E_x d + \sum_1^n A_{st} E_{st}\left(1 - \frac{y_n^2}{d^2}\right)\right]$$

$$+ \frac{\partial u_2}{\partial x} \partial\left(\frac{\delta u_0}{\partial x}\right)\left[\frac{2}{3} t E_x d + \sum_1^n A_{st} E_{st}\left(1 - \frac{y_n^2}{d^2}\right)\right]$$

$$+ \frac{\partial u_2}{\partial x} \partial\left(\frac{\delta u_2}{\partial x}\right)\left[\frac{8}{15} t E_x d + \sum_1^n A_{st} E_{st}\left(1 - \frac{y_n^2}{d^2}\right)^2\right]$$

$$+ \frac{4t}{3d} G u_2 \delta u_2 - \frac{b E_w h}{2} \frac{\partial u_0}{\partial x} \partial\left(\frac{\delta u_1}{\partial x}\right) - \frac{b E_w h}{2} \frac{\partial u_1}{\partial x} \partial\left(\frac{\delta u_0}{\partial x}\right)$$

$$\left. + \frac{b E_w h}{3} \frac{\partial u_1}{\partial x} \partial\left(\frac{\delta u_1}{\partial x}\right) - \frac{1}{2h} M_x \partial\left(\frac{\delta u_1}{\partial x}\right) \right\} dx$$

$$= 0$$

Let

$$\varphi_1 = t\,E_x\,d + b\,E_w h + \sum_1^n A_{st}\,E_{st}$$

$$\varphi_2 = \frac{2}{3}\,t\,E_x\,d + \sum_1^n A_{st}\,E_{st}\left(1 - \frac{y_n^2}{d^2}\right)$$

$$\varphi_3 = \frac{2}{3}\,t\,E_x\,d + \sum_1^n A_{st}\,E_{st}\left(1 - \frac{y_n^2}{d^2}\right)$$

$$\varphi_4 = \frac{8}{15}\,t\,E_x\,d + \sum_1^n A_{st}\,E_{st}\left(1 - \frac{y_n^2}{d^2}\right)^2$$

Integrating by parts gives

$$\left[\varphi_1 \frac{\partial u_0}{\partial x} \delta u_0 + \varphi_2 \frac{\partial u_0}{\partial x} \delta u_2 + \varphi_3 \frac{\partial u_2}{\partial x} \delta u_0 + \varphi_4 \frac{\partial u_2}{\partial x} \delta u_2 + \frac{b E_w h}{2}\left(-\frac{\partial u_0}{\partial x} \delta u_1 - \frac{\partial u_1}{\partial x} \delta u_0 + \frac{2}{3} \frac{\partial u_1}{\partial x} \delta u_1\right) + \frac{1}{2h} M_x \delta u_1\right]_0^L$$

$$- \int_0^L \left[\varphi_1 \frac{\partial^2 u_0}{\partial x^2} \delta u_0 + \varphi_2 \frac{\partial^2 u_0}{\partial x^2} \delta u_2 + \varphi_3 \frac{\partial^2 u_2}{\partial x^2} \delta u_0 + \varphi_4 \frac{\partial^2 u_2}{\partial x^2} \delta u_2 - \frac{4t}{3d} G u_2 \delta u_2 + \frac{b E_w h}{2}\left(-\frac{\partial^2 u_0}{\partial x^2} \delta u_1 - \frac{\partial^2 u_1}{\partial x^2} \delta u_0 + \frac{2}{3} \frac{\partial^2 u_1}{\partial x^2} \delta u_1\right) - \frac{1}{2h} \frac{\partial M}{\partial x} \delta u_1\right] dx = 0$$

The first bracket is equal to zero from the following assigned boundary conditions: At $x = L$,

$$\delta u_0 = \delta u_1 = \delta u_2 = 0$$

and at $x = 0$,

$$\frac{\partial u_0}{\partial x} = \frac{\partial u_1}{\partial x} = \frac{\partial u_2}{\partial x} = M_x = 0$$

The integral thus becomes

$$\int_0^L \left[\left(\varphi_1 \frac{\partial^2 u_0}{\partial x^2} + \varphi_3 \frac{\partial^2 u_2}{\partial x^2} - \frac{b E_w h}{2} \frac{\partial^2 u_1}{\partial x^2} \right) \delta u_0 \right.$$

$$+ \left(- \frac{b E_w h}{2} \frac{\partial^2 u_0}{\partial x^2} + \frac{b E_w h}{3} \frac{\partial^2 u_1}{\partial x^2} - \frac{1}{2h} \frac{\partial M}{\partial x} \right) \delta u_1$$

$$\left. + \left(\varphi_2 \frac{\partial^2 u_0}{\partial x^2} + \varphi_4 \frac{\partial^2 u_2}{\partial x^2} - \frac{4t}{3d} G u_2 \right) \delta u_2 \right] dx = 0$$

Since δu_1, δu_2, and δu_0 are arbitrary,

$$\varphi_1 \frac{\partial^2 u_0}{\partial x^2} + \varphi_3 \frac{\partial^2 u_2}{\partial x^2} - \frac{b E_w h}{2} \frac{\partial^2 u_1}{\partial x^2} = 0$$

$$- \frac{b E_w h}{2} \frac{\partial^2 u_0}{\partial x^2} + \frac{b E_w h}{3} \frac{\partial^2 u_1}{\partial x^2} - \frac{1}{2h} \frac{\partial M}{\partial x} = 0$$

$$\varphi_2 \frac{\partial^2 u_0}{\partial x^2} + \varphi_4 \frac{\partial^2 u_2}{\partial x^2} - \frac{4t}{3d} G u_2 = 0$$

Let

$$\lambda_1 = \frac{2\varphi_1}{b E_w h}$$

$$\lambda_2 = \frac{2\varphi_3}{b E_w h}$$

$$\lambda_3 = \frac{3\ d\varphi_2}{4t\ G}$$

$$\lambda_4 = \frac{3\ d\varphi_4}{4t\ G}$$

$$\lambda_5 = -\frac{1}{b\ E_w h^2}$$

Then

$$\left.\begin{aligned} \lambda_1 \frac{\partial^2 u_0}{\partial x^2} + \lambda_2 \frac{\partial^2 u_2}{\partial x^2} - \frac{\partial^2 u_1}{\partial x^2} &= 0 \\ -\frac{\partial^2 u_0}{\partial x^2} + \frac{2}{3} \frac{\partial^2 u_1}{\partial x^2} + \lambda_5 \frac{\partial M}{\partial x} &= 0 \\ \lambda_3 \frac{\partial^2 u_0}{\partial x^2} + \lambda_4 \frac{\partial^2 u_2}{\partial x^2} - u_2 &= 0 \end{aligned}\right\} \qquad (15)$$

By eliminating u_0, the following equation is obtained:

$$\left.\begin{aligned} \lambda_2 \frac{\partial^2 u_2}{\partial x^2} + \left(\frac{2}{3}\lambda_1 - 1\right) \frac{\partial^2 u_1}{\partial x^2} + \lambda_1 \lambda_5 \frac{\partial M}{\partial x} &= 0 \\ \lambda_4 \frac{\partial^2 u_2}{\partial x^2} + \frac{2}{3}\lambda_3 \frac{\partial^2 u_1}{\partial x^2} - u_2 + \lambda_3 \lambda_5 \frac{\partial M}{\partial x} &= 0 \end{aligned}\right\} \qquad (16)$$

Again, by eliminating u_1, the following equation is obtained:

$$\left[\lambda_4\left(\frac{2}{3}\lambda_1 - 1\right) - \frac{2}{3}\lambda_2\lambda_3\right]\frac{\partial^2 u_2}{\partial x^2} - \left(\frac{2}{3}\lambda_1 - 1\right)u_2 = \lambda_5\lambda_3\frac{\partial M}{\partial x}$$

By introducing the parameters ϕ_1 and ϕ_2 as follows

$$\phi_1^2 = \frac{\frac{2}{3}\lambda_1 - 1}{\lambda_4\left(\frac{2}{3}\lambda_1 - 1\right) - \frac{2}{3}\lambda_2\lambda_3}$$

$$\phi_2 = \frac{\lambda_3\lambda_5\frac{\partial M}{\partial x}}{\lambda_4\left(\frac{2}{3}\lambda_1 - 1\right) - \frac{2}{3}\lambda_2\lambda_3}$$

the final differential equation is obtained

$$\frac{\partial^2 u_2}{\partial x^2} - \phi_1^2 u_2 = \phi_2 \tag{17}$$

On assuming ϕ_2 equal to a positive constant, the solution is

$$u_2 = C_1 \sinh \phi_1 x + C_2 \cosh \phi_1 x - \frac{\phi_2}{\phi_1^2} \tag{18}$$

The constants of integration are determined as follows: At $x = 0$,

$$\frac{\partial u_2}{\partial x} = 0$$

therefore $C_1 = 0$. At $x = L$,

$$u_2 = 0$$

therefore

$$C_2 = \frac{\phi_2}{\phi_1^2 \cosh \phi_1 L}$$

Consequently,

$$u_2 = \frac{\phi_2}{\phi_1^2}\left(\frac{\cosh \phi_1 x}{\cosh \phi_1 L} - 1\right) \tag{19}$$

Substituting u_2 and $\frac{\partial^2 u_2}{\partial x^2}$ into the third equation of equation (15) yields

$$\frac{\partial^2 u_0}{\partial x^2} = \frac{\phi_2}{\lambda_3 \phi_1^2}\left(\frac{\cosh \phi_1 x}{\cosh \phi_1 L} - 1\right) - \frac{\lambda_4 \phi_2}{\lambda_3} \frac{\cosh \phi_1 x}{\cosh \phi_1 L} \tag{20}$$

$$\frac{\partial u_0}{\partial x} = \frac{\phi_2}{\lambda_3 \phi_1^3} \frac{\sinh \phi_1 x}{\cosh \phi_1 L} - \frac{\lambda_4 \phi_2}{\lambda_3 \phi_1} \frac{\sinh \phi_1 x}{\cosh \phi_1 L} - \frac{\phi_2 x}{\lambda_3 \phi_1^2} + C_3 \tag{21}$$

$$u_0 = \frac{\phi_2}{\lambda_3 \phi_1^4} \frac{\cosh \phi_1 x}{\cosh \phi_1 L} - \frac{\lambda_4 \phi_2}{\lambda_3 \phi_1^2} \frac{\cosh \phi_1 x}{\cosh \phi_1 L} - \frac{\phi_2 x^2}{2\lambda_3 \phi_1^2} + C_3 x + C_4 \tag{22}$$

At $x = 0$,

$$\frac{\partial u_0}{\partial x} = 0$$

therefore $C_3 = 0$. At $x = L$,

$$u_0 = 0$$

Therefore

$$C_4 = -\frac{\phi_2}{\lambda_3 \phi_1^4} + \frac{\lambda_1 \phi_2}{\lambda_3 \phi_1^2} + \frac{\phi_2 L^2}{2\lambda^3 \phi_1^2}$$

Substituting into equation (22) gives

$$u_0 = \frac{\phi_2}{\lambda_3 \phi_1^2}\left(\frac{1}{\phi_1^2} - \lambda_4\right)\frac{\cosh \phi_1 x}{\cosh \phi_1 L} - \frac{\phi_2}{\lambda_3 \phi_1^2}\left(\frac{1}{\phi_1^2} - \lambda_4\right) + \frac{\phi_2}{2\lambda_3 \phi_1^2}(L^2 - x^2) \quad (23)$$

From equations (19) and (23),

$$\frac{\partial u_2}{\partial x} = \frac{\phi_2}{\phi_1}\frac{\sinh \phi_1 x}{\cosh \phi_1 L}$$

$$\frac{\partial u_0}{\partial x} = \frac{\phi_2}{\lambda_3 \phi_1}\left[\left(\frac{1}{\phi_1} - \lambda_4\right)\frac{\sinh \phi_1 x}{\cosh \phi_1 L} - \frac{x}{\phi_1}\right]$$

Consequently, from equation (7), the strain is obtained as follows:

$$\epsilon_x = \frac{\phi_2}{\lambda_3 \phi_1}\left[\left(\frac{1}{\phi_1^2} - \lambda_4\right)\frac{\sinh \phi_1 x}{\cosh \phi_1 L} - \frac{x}{\phi_1}\right] + \left(1 - \frac{y^2}{d^2}\right)\frac{\phi_2}{\phi_1}\frac{\sinh \phi_1 x}{\cosh \phi_1 L} \quad (24)$$

and from equations (8) and (19),

$$\gamma_{xy} = \frac{2y}{d^2}\frac{\phi_2}{\phi_1}\left(1 - \frac{\cosh \phi_1 x}{\cosh \phi_1 L}\right) \quad (25)$$

DESCRIPTION OF TEST

For the purpose of studying the shear-lag effect and stress-strain distribution on a thin plywood sheet reinforced by longitudinal stringers used for the chord member of a box beam, the test specimen shown in figure 2 was built and tested as a simple beam loaded at midspan.

Test Specimen

The beam was 96 inches long, 32 inches wide, and 6 inches deep, open on one side and covered on the other by a plywood sheet-stringer combination. The box beam itself was reinforced by eight transverse wood stiffeners spaced 12 inches apart and four steel rods, in order to eliminate lateral deflection. (See fig. 2.) Five longitudinal stringers spaced 5 inches apart were used for the plywood sheet-stringer combination.

The side members were rectangular beams of California sugar pine, one with 6- by 2-inch and the other with 6- by $1\frac{3}{4}$-inch cross sections. Their widths were made inversely proportional to their respective moduli of elasticity to meet the condition of elastic symmetry for the composite box beam.

The chord member was a sheet-stringer combination consisting of five $\frac{3}{4}$- by $\frac{3}{4}$-inch longitudinal stringers of California sugar pine glued on one face of a sheet of plywood of 0.07-inch thickness. The plywood sheet was composed of two 0.02-inch mahogany face plies and one 0.03-inch core of yellow poplar with the grain of the core and face plies at right angles to each other.

The transverse stiffeners were 2- by 2-inch pieces of California sugar pine. The steel rods were of $\frac{3}{8}$-inch diameter fastened at their ends by screws and nuts. All component parts except the steel rods were glued together, with the face grain of the plywood sheet making an angle of 45° with the longitudinal axis of the composite box beam.

Arrangement for Loading

The system of loading was arranged to represent a simple beam with a concentrated load applied at midspan. The testing machine consists essentially of two pairs of jacks, individually operated, to deflect the ends of the beam, and of a yoke around its center connected to a lever balance system to measure the necessary reaction force (fig. 3). For

the purpose of assuring an evenly applied load, however, one pair of the jacks was replaced by a stationary end support. (This alteration was only permissible under the assumption of very small deflection which, in the present case, amounts to only 0.003 percent of the length of the beam.) The arrangement is shown in figures 3 and 4.

The load was applied by operating the two screw jacks and their relative motion was checked by spirit levels. Steel blocks with rounded heads were used to approximate a line load; steel plates were used to avoid crushing of wood at the point of application of the load. Details of the loading device are shown in figure 4.

Arrangement for Measurement of Strain

The strains were measured by means of electrical-resistance strain gages connected with a portable strain indicator. Two different types of gage were used: plain gages for measuring strains in only one direction, and rosette gages for measuring strains in three directions at 45° to each other. The strains were read in microinches per inch directly from the strain indicator. Other details of these gages are shown in reference 5.

The strain gages were attached to plywood and stringers along three different transverse sections, as shown in figures 5 and 6. This arrangement was decided upon in order to study the following characteristics: high shear strains at section 1 (24 in. from midspan), appreciable shear and normal strains at section 2 (12 in. from midspan), and zero shear strain with high normal strains at section 3 (at midspan).

Rosette gages were placed between longitudinal stringers to measure both normal and shear strains, whereas plain gages were located at the places where only normal strains were to be measured. Gages were closely disposed on both faces of section 2 to provide a thorough check of theory. However, at section 3 where zero shear strain was expected, 13 plain gages and only 3 rosette gages were used. Theoretically, maximum shear would have appeared at sections near the end of the beam; hence rosette gages were used at section 1 to check this phenomenon. (Local irregularities at sections nearer the free edge would make reasonable readings impossible.)

The strain gages were connected to the strain indicators by means of a switch box to facilitate reading. (See fig. 7.) For every loading, corresponding strain readings of all the strain gages were taken. The initial zero load strain readings were checked after every series of loadings. The strain gages were divided into two groups and readings were taken simultaneously with two individual strain indicators. This scheme was arranged to reduce the time required for taking readings, thus reducing the possible influence of creep.

Procedure of Test

The beam was loaded by successive 200-pound increments of loads of: (1) from 0 to 400 pounds, (2) from 0 to 800 pounds, (3) from 0 to 1200 pounds, and (4) from 0 to 2000 pounds.

DISCUSSION OF RESULTS

A very satisfactory agreement between the theoretical and experimental results for both normal and shearing strains was obtained. The maximum difference of strains between experimental and theoretical results (tables 1 and 2) was found to be about 15 percent of the experimental value; because of the nonhomogeneity of wooden structures, this result is likely to be about the best obtainable.

The comparative results were plotted as shown in figures 8 to 13. By plotting the experimental normal strains for sections 2 and 3 (figs. 9 and 10), local shear-lag effects on the sheet between the longitudinal stringers were observed. This effect was to be expected, yet it was not taken into account in the theory. To have done so would have complicated the mathematics considerably. The distribution of experimental shearing strains resembles a cubic parabola, whereas the theoretical curve is a straight line (figs. 9 and 10). Nevertheless, the agreement is very good so far as the maximum values are concerned. The other points on the curves show the theoretical results to be conservative as to magnitude of stresses.

In figures 12 and 13, comparative normal strain distributions on stringers were plotted. In the development of the theory, it was assumed that the centroids of the stringers coincided with the midplane of the sheet. However, in practical construction this is never true. Thus a local bending effect of the stringers was to be expected, the result of which was that strains on the free face of the stringers were of a much lower value than those on the face to which the plywood was glued. A relation between them can be obtained as follows.

If the stringer is considered as a small cantilever beam subjected to a horizontal load of p pounds per inch acting on one of the faces, as shown in figure 14, and if the vertical component of p which appears as a result of the bending deformation of the stringer is neglected by considering that the bending modulus of elasticity of the sheet is negligible, the normal force and the bending moment at any section can be given by the following expressions:

$$dN_x = p\,dx$$

$$N_x = \int_0^x p\,dx$$

$$dM_x = a\ p\ dx$$

$$M_x = \int_0^x a\ p\ dx = a \int_0^x p\ dx$$

But

$$f_{xa} = \frac{M_x a}{I} + \frac{N_x}{A}$$

$$f_{xb} = \frac{M_x b}{I} - \frac{N_x}{A}$$

where f_{xa} and f_{xb} are stresses.

For constant section and constant E the ratio of strains is given by

$$\frac{e_{xb}}{e_{xa}} = \frac{f_{xb}}{f_{xa}} = \frac{\frac{M_x b}{I} - \frac{N_x}{A}}{\frac{M_x a}{I} + \frac{N_x}{A}} = \frac{\frac{ab}{I} - \frac{1}{A} \int_0^x p\ dx}{\frac{a^2}{I} + \frac{1}{A} \int_0^x p\ dx}$$

Hence, for symmetrical sections,

$$\frac{e_{xb}}{e_{xa}} = \frac{\frac{ab}{I} - \frac{1}{A}}{\frac{a^2}{I} + \frac{1}{A}} < 1$$

For the particular case of rectangular stringer $a = b = \frac{h}{2}$, $I = \frac{dh^3}{12}$, and $A = dh$,

$$\frac{e_{xb}}{e_{xa}} = \frac{\frac{h^2 \times 12}{4 \times dh^3} - \frac{1}{dh}}{\frac{h^2 \times 12}{4 \times dh^3} + \frac{1}{dh}} = \frac{\frac{2}{dh}}{\frac{4}{dh}} = \frac{1}{2}$$

Although the relation $\frac{e_{xb}}{e_{xa}} < 1$ has been confirmed, the experimental results showed a large discrepancy from the relation $\frac{e_{xb}}{e_{xa}} = \frac{1}{2}$, especially for the central stringers. For design purposes, the maximum strain on the stringer can be assumed equal to that on the sheet.

CONCLUSION

The theoretical and experimental investigation of shear-lag action presented is based on the concept of an idealized structure in which the main sources of strain energy of the real structure are maintained while the secondary sources are neglected, and thus the idealized chord member has infinite rigidity in the transverse direction.

The test results justify the adequacy of the theory for practical design, because the differences between theoretical and experimental results in the critical regions are smaller than would be expected from the usually irregular behavior of practical structures made of wood and plywood.

Massachusetts Institute of Technology
Cambridge, Mass., August 5, 1947

APPENDIX - EVALUATION OF PROPERTIES

Determination of Bending Modulus of Elasticity of Side Members

In order to determine the bending modulus of elasticity of the side members, a transverse bending test was performed (fig. 15). The specimen was tested as a simple beam, supported near the ends and loaded at midspan. The tests were run with the specimen in normal position and with it turned over. Deflections at midspan were measured by means of a dial gage. Load-deflection curves were plotted and from them the bending modulus of elasticity was computed. A correction term for deflection due to shear was included in the formula for E.

The average values for the modulus of elasticity were found to be:

Beam I.....1,782,000 psi

Beam II.....2,026,000 psi

Determination of Tension Modulus of Elasticity of Longitudinal Stringers

The value of E for the longitudinal stringers was determined from tension tests on specimens having the dimensions shown in figure 15. The specimens were cut from three individual longitudinal stringers, the longitudinal axes of which were parallel to wood grain. Tension loads were applied with the ends of the specimen attached by tightly clamped steel plates. Strains were measured by electrical-resistance strain gages with strain indicators, and Huggenberger tensometers were set on both sides of the test specimen for check readings.

Load-strain curves were plotted, from the slopes of which E was computed. The average value for the three specimens was found to be 1,496,000 psi.

Determination of Modulus of Elasticity and Poisson's Ratio for Plywood

Modulus of elasticity and Poisson's ratio were determined by tension tests similar to that outlined for determination of E for longitudinal stringers. A simple bolted joint was used at the ends of the specimen. Electrical-resistance strain gages were glued parallel to the axis of

loading on one face and perpendicular on the opposite face of the specimen to measure longitudinal and lateral strains. The specimens were cut out of the same sheet used for the composite box beam. The sizes were as shown in figure 16, with the longitudinal axis parallel, perpendicular, and at a 45° angle with the face grains. Load-strain curves were plotted from which the data on modulus of elasticity and Poisson's ratio were computed.

The reading from the longitudinal gage is affected by transverse strain and that from the lateral gage is affected by longitudinal strain. In order to take into account these effects, the formula for rosette strain gages was applied, and longitudinal and lateral strains were obtained from

$$\epsilon_L = e_1 - \frac{e_3}{55}$$

$$\epsilon_T = e_3 - \frac{e_1}{55}$$

where

e_1 longitudinal strain-gage reading

e_3 transverse strain-gage reading

Since e_3 is always small compared with e_1, the second term could be neglected in the formula for ϵ_L and E computed directly from e_1 readings.

$$E = \frac{P/A}{\epsilon_L} = \frac{P/A}{e_1}$$

However, the effect of longitudinal strain on lateral strain is of an appreciable amount; consequently Poisson's ratio must be computed by

$$J = -\frac{\epsilon_T}{\epsilon_L} = -\frac{e_T - \frac{e_L}{55}}{e_L} = -\frac{e_T}{e_L} + 0.02$$

From the tests,

$$J_{uv} = 0.1152$$

$$J_{vu} = 0.1189$$

$$E_u = 875,000$$

$$E_v = 837,000$$

Determination of Modulus of Rigidity for Plywood

Based on a well-known result in the theory of bending of thin plates (reference 6), a method of determining modulus of rigidity was outlined in reference 7. The method consists in determining the deflection of a square plywood plate loaded at two opposite corners and supported at the other two. The deflections were measured at points on the diagonals equally distant from the center. Load-deflection curves were plotted, from the slopes of which the modulus of rigidity was determined from the formula

$$G = \frac{3}{2} \frac{u^2}{h^3} \frac{P}{w}$$

where

P load on each corner

w deflection of points on diagonal relative to center of plate

u distance from center to points on diagonal

h thickness of plate

The specimens used were 3- by 3-inch and $2\frac{1}{2}$- by $2\frac{1}{2}$-inch sizes and their edges were either parallel or perpendicular to the face grains. Small thin copper sheets were glued on the corners in order to eliminate local stress effects at load points.

The deflections were measured by means of dial gages. The load was applied by a testing machine as shown in figure 17. Effects on dial

reading caused by initial curvature and gage spring force were minimized by obtaining two sets of readings for each specimen, one with the loads acting downward on two specified opposite corners, the other with the specimen rotated through 90° so that the loads acted upward on these corners. At the same time, dial gages were carefully chosen so that their spring forces were about equal.

From the tests, the following results were obtained:

	3- by 3-inch specimens	$2\frac{1}{2}$- by $2\frac{1}{2}$-inch specimens
G_{uv}	140,300 psi	139,300 psi

An average of five specimens gave a value of G_{uv} of 139,900 psi.

Stress-Strain Relations for Plywood at Any Angle to the Grain

It is usually assumed that plywood behaves elastically as an orthotropic material. The axes parallel and perpendicular to the grain are generally taken as principal axes of strains.

Let E_u and E_v be the moduli of elasticity in the directions parallel and perpendicular to the face grain; J_{vu} and J_{uv}, the Poisson's ratios in those directions; and G_{uv}, the modulus of rigidity referred to shearing stresses parallel and perpendicular to the axes u and v, respectively.

With x and y indicating directions at 45° to the face grains,

$$\left.\begin{aligned} E_x = E_y &= \left(\frac{1}{4}\,\frac{1 - J_{uv}}{E_u} + \frac{1 - J_{vu}}{E_v} + \frac{1}{G_{uv}}\right) \\ J_{xy} = J_{yx} &= \frac{\dfrac{1}{G_{uv}} - \dfrac{1 - J_{uv}}{E_u} - \dfrac{1 - J_{vu}}{E_v}}{\dfrac{1}{G_{uv}} + \dfrac{1 - J_{uv}}{E_u} + \dfrac{1 - J_{vu}}{E_v}} \\ \frac{1}{G_{xy}} &= \frac{1 + J_{uv}}{E_u} + \frac{1 + J_{vu}}{E_v} \end{aligned}\right\} \qquad (26)$$

A derivation of these relations can be found in references 2, 8, and 9.

From the tests, it was found that E_{xy} = 546,000 and 555,000, J_{xy} = 0.520 and 0.609, and G_{xy} = 383,000.

COMPARATIVE VALUES BASED ON DATA FROM REFERENCE 10

[L indicates parallel to grain; T indicates perpendicular to grain]

	Mahogany	Yellow poplar
E_L(psi)	1,380,000	1,430,000
E_T/E_L	0.039	0.039
E_T(psi)	54,000	52,000
J_{TL}	0.552	0.406
G_{LT}/E	0.038	0.053
G_{LT}(psi)	53,500	76,000

$$E_u = \frac{1}{t}\left(t_2E_{Lm} + t_1E_{Tp}\right) = \frac{1}{7}\left[(4 \times 1380) + (3 \times 52)\right] \times 1000$$

$$= 811{,}000 \text{ psi}$$

$$E_v = \frac{1}{t}\left(t_2E_{Tm} + t_1E_{Lp}\right) = \frac{1}{7}\left[(4 \times 54) + (3 \times 1430)\right] \times 1000$$

$$= 644{,}000 \text{ psi}$$

$$J_{vu} = \frac{1}{tE_v}\left(t_2E_{Tm}J_{LTm} + t_1E_{Lp}J_{TLp}\right)$$

$$= \frac{1}{7 \times 644}\left[(4 \times 54 \times 0.552) + (3 \times 1430 \times 0.020)\right] = 0.0455$$

$$J_{uv} = \frac{1}{tE_u}\left(t_2E_{Lm}J_{TLm} + t_1E_{Tp}J_{LTp}\right)$$

$$= \frac{1}{7 \times 811}\left[(4 \times 1380 \times 0.0215) + (3 \times 52 \times 0.406)\right] = 0.0322$$

$$G_{uv} = \frac{1}{t}\left(t_2 G_m + t_1 G_p\right)$$

$$= \frac{1}{7}\left[(4 \times 53.5) + (3 \times 76)\right] \times 1000 = 63{,}200 \text{ psi}$$

$$\frac{1}{E_x} = \frac{1}{E_y} = \frac{1 - J_{uv}}{4\,E_u} + \frac{1 - J_{vu}}{4\,E_v} + \frac{1}{4\,G_{uv}}$$

$$= \frac{1 - 0.0322}{4 \times 811{,}000} + \frac{1 - 0.0455}{4 \times 644{,}000} + \frac{1}{4 \times 63{,}200} = 4.626 \times 10^{-6}$$

$$E_x = E_y = 216{,}000 \text{ psi}$$

$$J_{xy} = J_{yx} = \frac{\dfrac{1}{G_{uv}} - \dfrac{1 - J_{uv}}{E_u} - \dfrac{1 - J_{vu}}{E_v}}{\dfrac{1}{G_{uv}} + \dfrac{1 - J_{uv}}{E_u} + \dfrac{1 - J_{vu}}{E_v}}$$

$$= \frac{\dfrac{1}{63.2} - \dfrac{1 - 0.0322}{811} - \dfrac{1 - 0.0455}{644}}{\dfrac{1}{63.2} + \dfrac{1 - 0.0322}{811} + \dfrac{1 - 0.0455}{644}} = 0.712$$

$$\frac{1}{G_{xy}} = \frac{1 + J_{uv}}{E_u} + \frac{1 + J_{vu}}{E_v}$$

$$= \frac{1 + 0.0322}{811{,}000} + \frac{1 + 0.0455}{844{,}000} = 2.897 \times 10^{-6}$$

$$G_{xy} = 346{,}000 \text{ psi}$$

Check of Strain-Energy Relation $E_u J_{uv} = E_v J_{vu}$

	$E_u J_{vu}$	$E_v J_{vu}$	Difference	Error from mean value (percent)
Experimental value	100.6×10^3	99.6×10^3	1.0×10^3	1.0
Reference 10	26.1	29.3	3.2	11.6

The average or standard data given in reference 10 do not conform to the requirements of the strain-energy relation as well as the data from a limited number of tests on the material used in this beam. An effect of this sort would be expected, perhaps, but the actual discrepancy when the data of reference 10 are used is greater than would be anticipated.

SUMMARY OF ELASTIC PROPERTIES OF WOOD MEMBERS

	From experiment	Computed from experiment	Computed from data of reference 10	Difference from data of reference 10 (percent)
Side members (California sugar pine)				
E_1(psi)	1782×10^3	----------	1144×10^3	56.0
E_2(psi)	2026×10^3	----------	1144×10^3	72.0
Stringers (California sugar pine)				
E_{st}(psi)	1496×10^3	----------	1144×10^3	30.6
Plywood (mahogany; yellow poplar)				
E_u(psi)	875×10^3	----------	811×10^3	8.3
E_v(psi)	837×10^3	----------	644×10^3	14.4
J_{uv}	0.115	----------	0.0322	----------
J_{vu}	0.119	----------	0.0455	----------
G_{uv}(psi)	139.5×10^3	----------	----------	----------
E_{xy}(psi)	550.5×10^3	433×10^3	216×10^3	155
J_{xy}	0.565	0.553	0.712	-6.6
G_{xy}(psi)	----------	383×10^3	346×10^3	10.7

Because of the length of the tables recording the observed strains and of the computations of the theoretical strains, test data and computations are not recorded here. The reduction of the test readings was done by standard methods, by using the properties of wood obtained from experiment rather than those from reference 10. The theoretical values were computed from the procedure presented in the first part of this report, again by using the properties of the wood in this particular beam.

The curves of figures 8 to 13 show the agreement between theoretical and experimental strains when the values resulting from the computations are plotted. The agreement is, in general, satisfactory evidence of the accuracy of the computations which are not included here.

REFERENCES

1. Reissner, Eric: Analysis of Shear Lag in Box Beams by the Principle of Minimum Potential Energy. Quarterly Appl. Math., vol. IV, Oct. 1946, p. 268.

2. Love, A.E.H.: A Treatise on the Mathematical Theory of Elasticity. Fourth ed., Dover Pub. (New York), 1944.

3. Hildebrand, Francis B.: The Exact Solution of Shear-Lag Problems in Flat Panels and Box Beams Assumed Rigid in the Transverse Direction. NACA TN No. 894, 1943.

4. Reissner, Eric: Least Work Solutions of Shear Lag Problems. Jour. Aero. Sci., vol. 8, no. 7, May 1941, pp. 284-291.

5. Anon.: SR-4 Strain Gage. Bull. 164, Baldwin Southwark, Div. of The Baldwin Locomotive Works (Philadelphia).

6. Timoshenko, S.: Theory of Plates and Shells. McGraw-Hill Book Co., Inc., 1940.

7. March, H.W., Kuenzi, E.W., and Kommers, W.J.: Method of Measuring the Shearing Moduli in Wood. Mimeo. No. 1301, Forest Products Lab., U.S. Dept. Agriculture, June 1942.

8. Oliveira, O.H.B.: Shear Lag in Plywood Flat Sheet Used for Chord Member of Box-Beam. Thesis, M.I.T., 1943.

9. March, H.W.: Stress-Strain Relations in Wood and Plywood Considered as Orthotropic Materials. Mimeo. No. 1503, Forest Products Lab., U.S. Dept. Agriculture, Feb. 1944.

10. Anon.: Design of Wood Aircraft Structure. ANC-18 Handbook, 1944.

TABLE 1

THEORETICAL STRAINS

[For 1000 lb at midspan; for 500 lb at tip]

x (in. from free edge)	y (in.)	Sheet		Stringers	
		ϵ_x	γ_{xy}	ϵ_{st} (top)	ϵ_{st} (bottom)
12	0	64.01×10^{-6}	----------	64.01×10^{-6}	32.0×10^{-6}
	5	68.85	----------	68.85	34.42
	10	83.36	----------	83.36	41.68
	12.1875	92.74	-552.68×10^{-6}	----------	----------
	14	101.93	-634.87	----------	----------
22 (Section 1)	0	110.27	----------	110.27	55.13
	5	120.33	----------	120.33	60.16
	10	150.49	----------	150.49	75.25
	12.1875	170.01	-485.43	----------	----------
	14	189.10	-557.62	----------	----------
34 (Section 2)	0	146.19	----------	146.19	73.09
	5	165.80	----------	165.80	82.90
	10	224.60	----------	224.60	112.30
	12.1875	262.66	-316.37	----------	----------
	14	299.88	-363.42	----------	----------
46 (Section 3)	0	141.920	----------	141.920	70.96
	5	177.815	----------	177.82	88.91
	10	285.50	----------	285.50	142.75
	12.1875	355.18	0	----------	----------
	14	423.34	0	----------	----------

TABLE 2

EXPERIMENTAL STRAINS

[For 1000 lb at midspan; for 500 lb at tip]

Section	y (in.)	Sheet			Stringers	
		ϵ_x	ϵ_y	γ_{xy}	ϵ_{st} (top)	ϵ_{st} (bottom)
1	-12.1875	182.14×10^{-6}	-11.80×10^{-6}	-496.40×10^{-6}	----------	----------
	-7.5	147.35	-25.26	-201.03	----------	----------
	-2.5	145.31	-22.23	-15.28	----------	----------
2	-15	354	-70.36	-294.42	354×10^{-6}	----------
	-12.1875	229.64	----------	----------	----------	----------
	-10.0	270	----------	----------	270	176×10^{-6}
	-7.5	190.35	-25.67	-117.53	----------	----------
	-5	195	----------	----------	195	----------
	-2.5	138.76	10.16	-19.97	----------	----------
	0	164	----------	----------	164	-26
	2.5	137.26	10.19	8.05	----------	----------
	5.0	180	----------	----------	180	50
	7.5	191.30	-34.69	117.50	----------	----------
	10.0	264	----------	----------	264	81
	13.00	240.49	-35.69	302.40	----------	----------
	15.125	353	----------	----------	353	----------
3	-15	479	----------	----------	479	----------
	-12.1875	304.53	-73.85	-16.33	----------	----------
	-10	300	----------	----------	300	183
	-7.5	205.15	-22.08	13.13	----------	----------
	-5	202	----------	----------	202	54
	-2.5	152.23	32.62	4.02	----------	----------
	0	160	----------	----------	160	-17
	5	193	----------	----------	193	----------
	10	219	----------	----------	291	----------
	15.125	472	----------	----------	472	----------

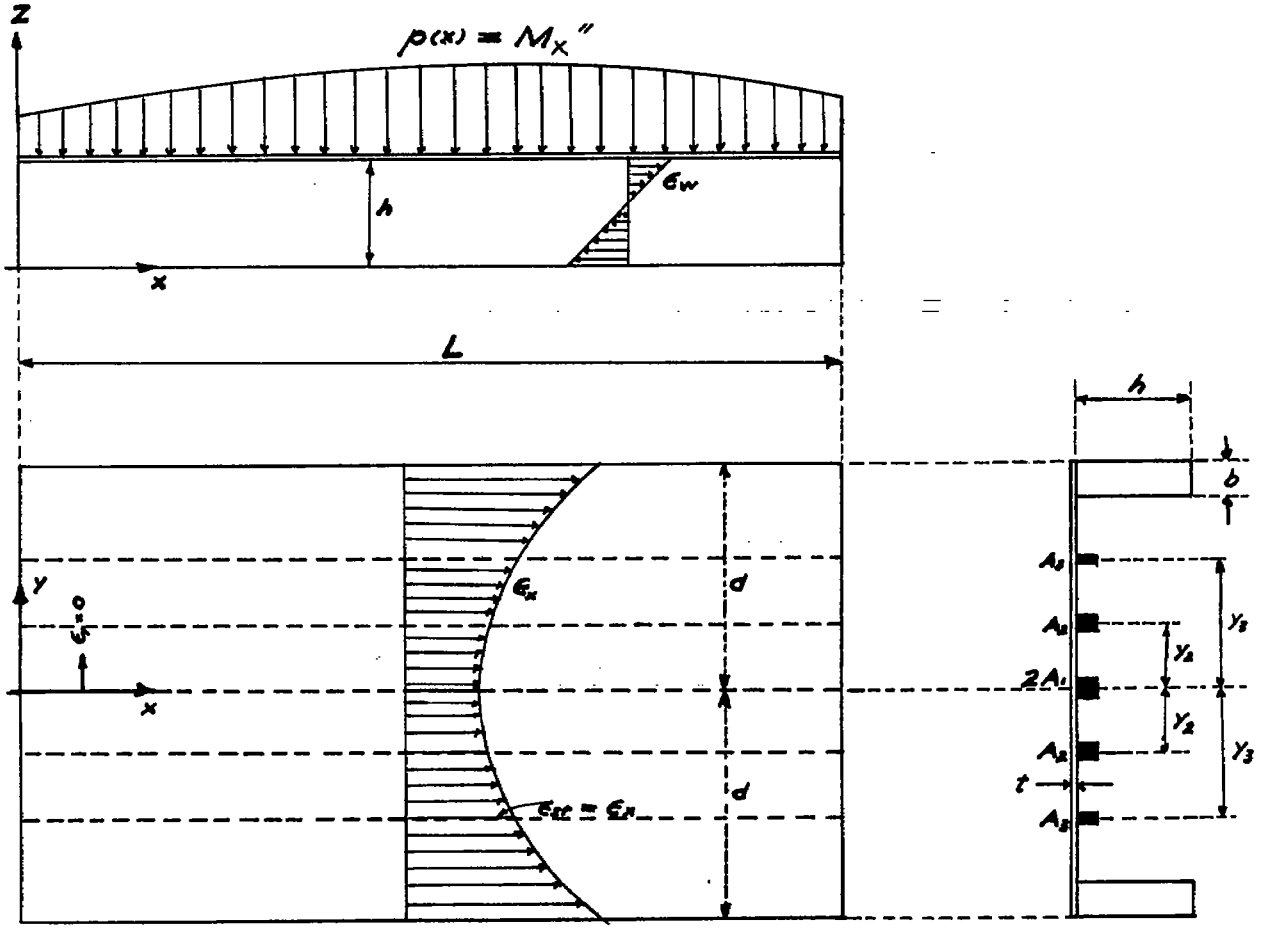

Figure 1.- Symbols used in the theory.

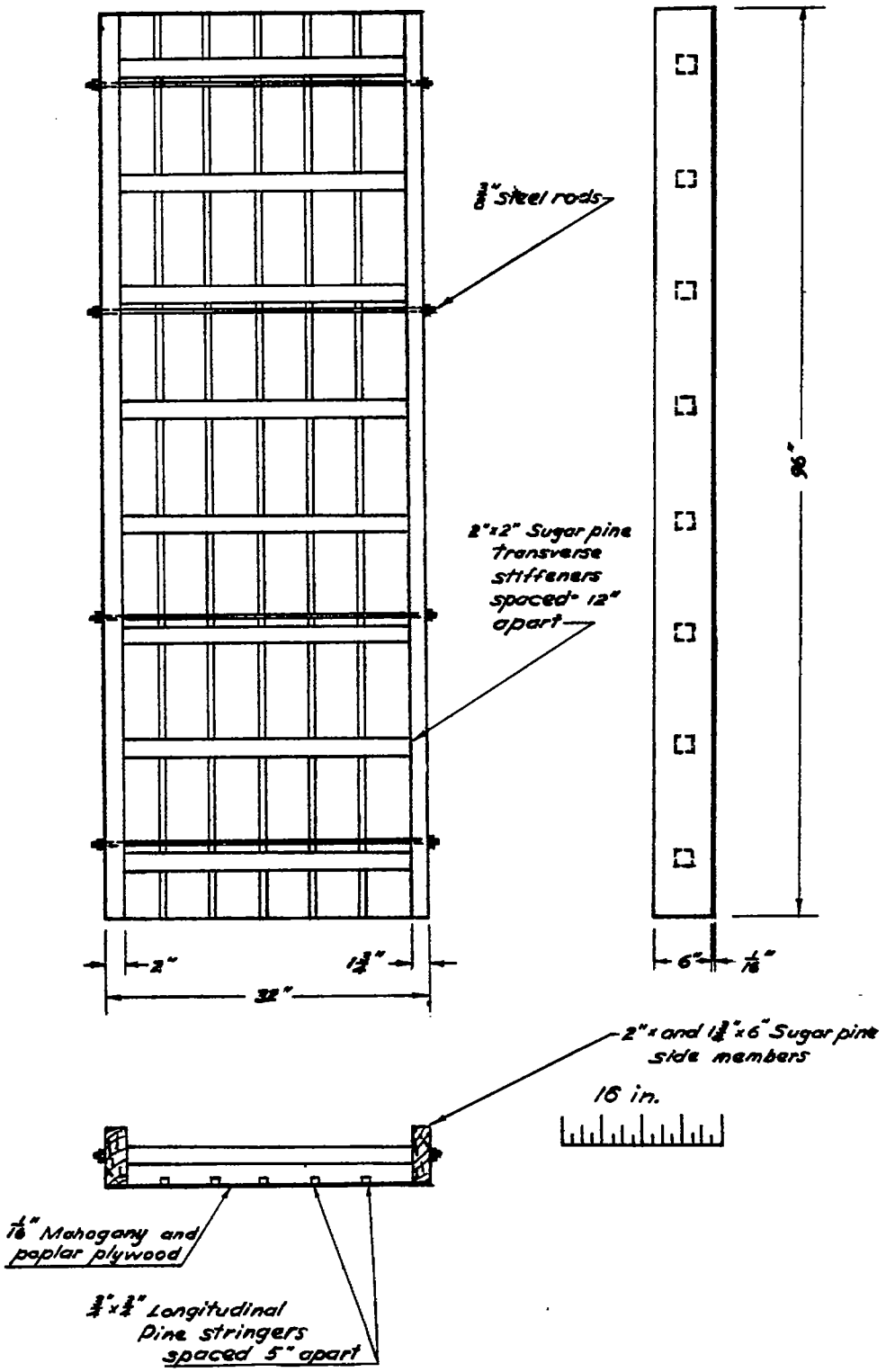

Figure 2.- Test beam.

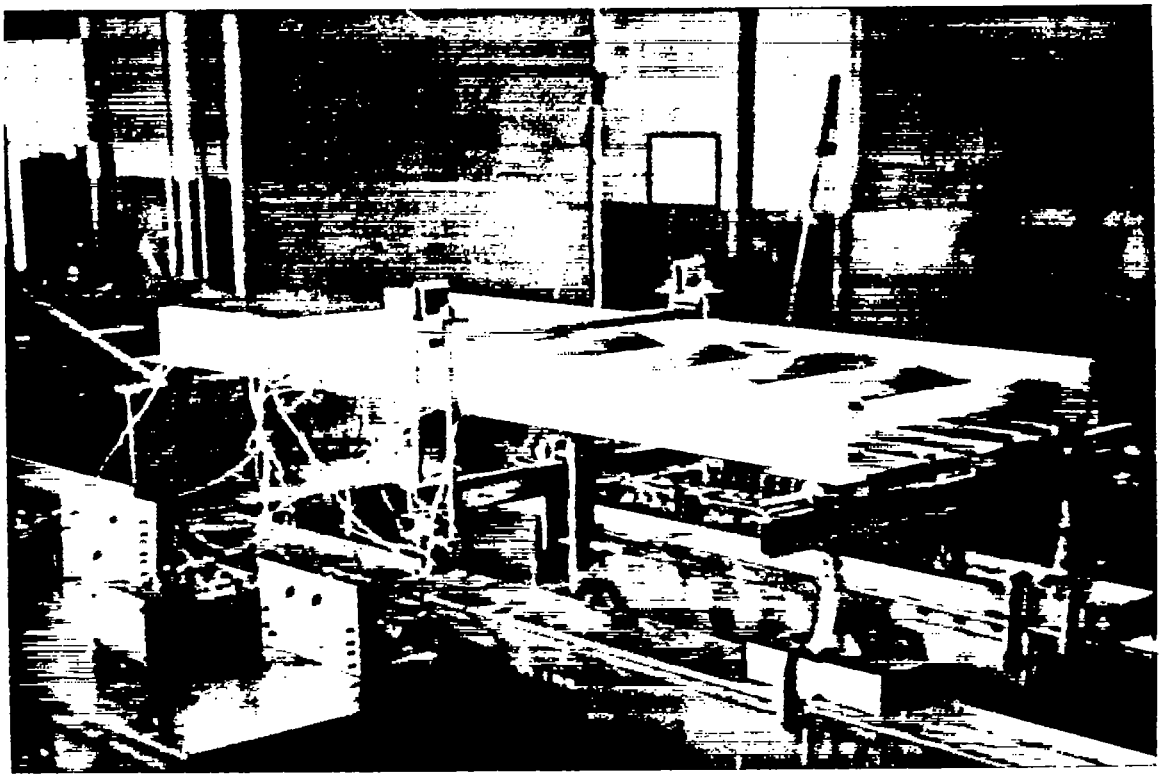

Figure 3.- Beam ready for test.

Figure 4.- Detail of loading device.

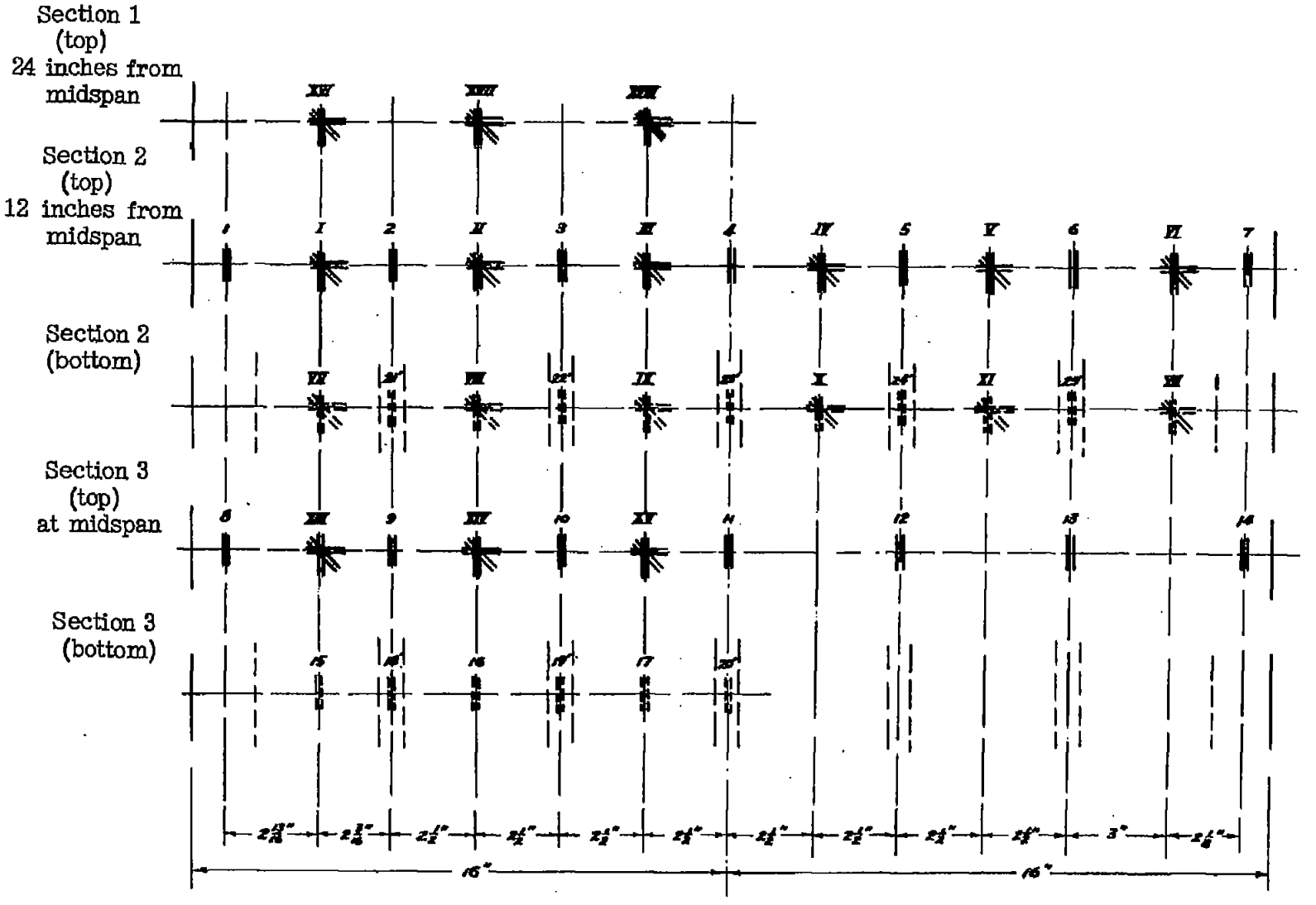

Figure 5.- Location of strain gages.

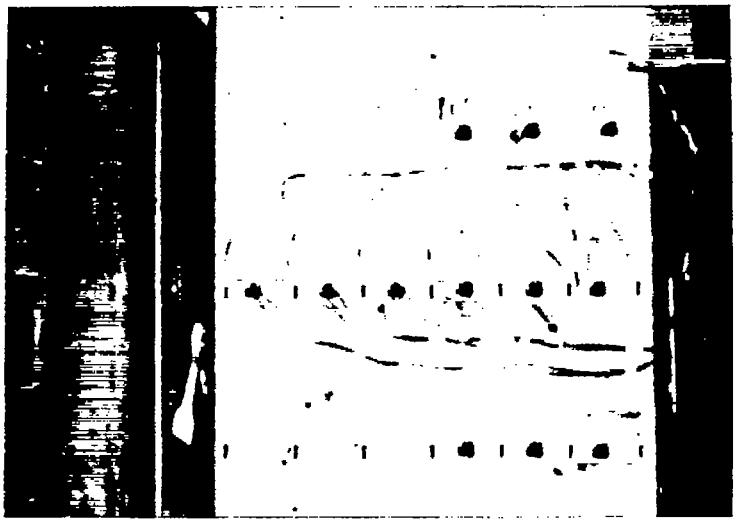

(a) Top.

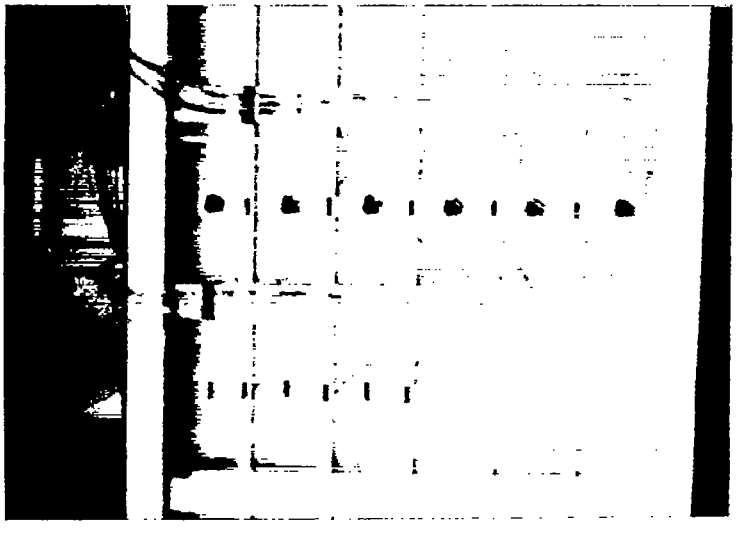

(b) Bottom.

Figure 6.- Location of strain gages.

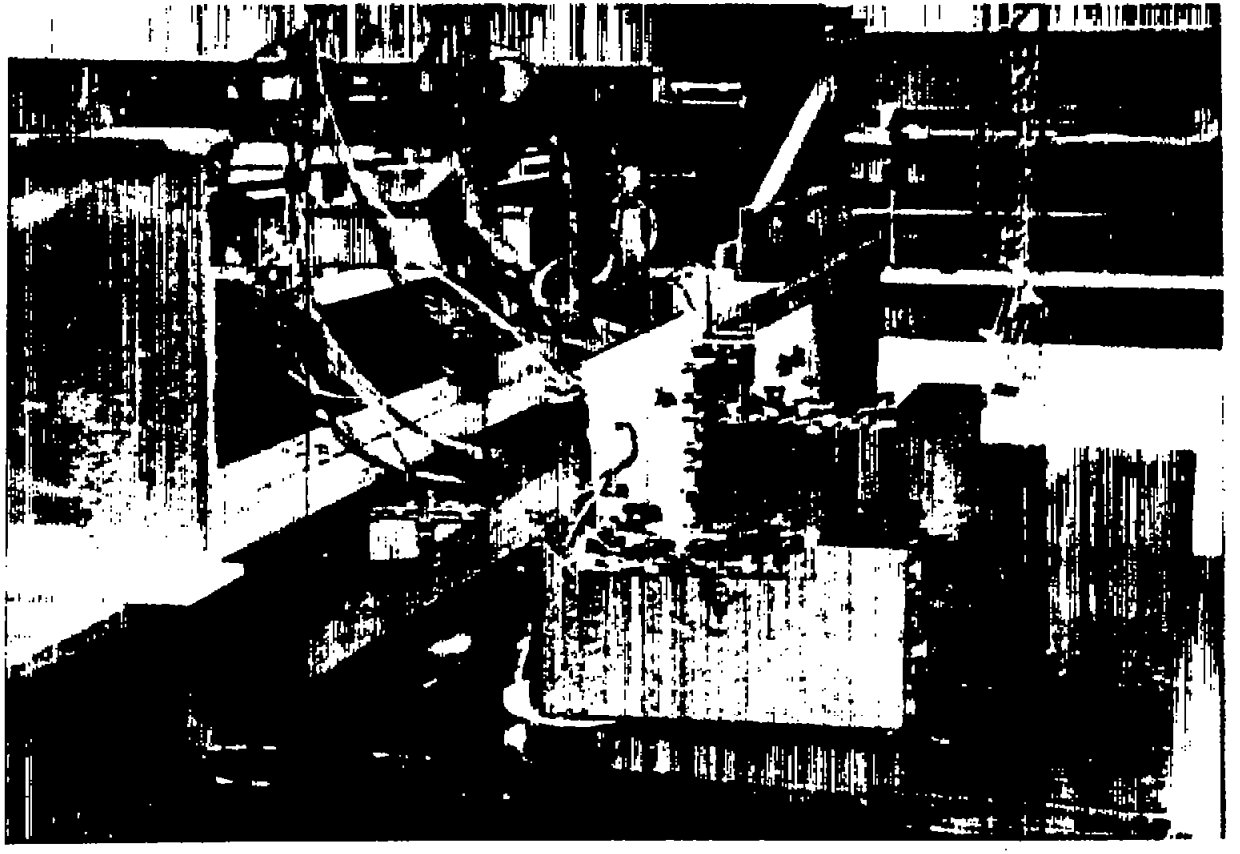

Figure 7.- Strain indicators and switch boxes.

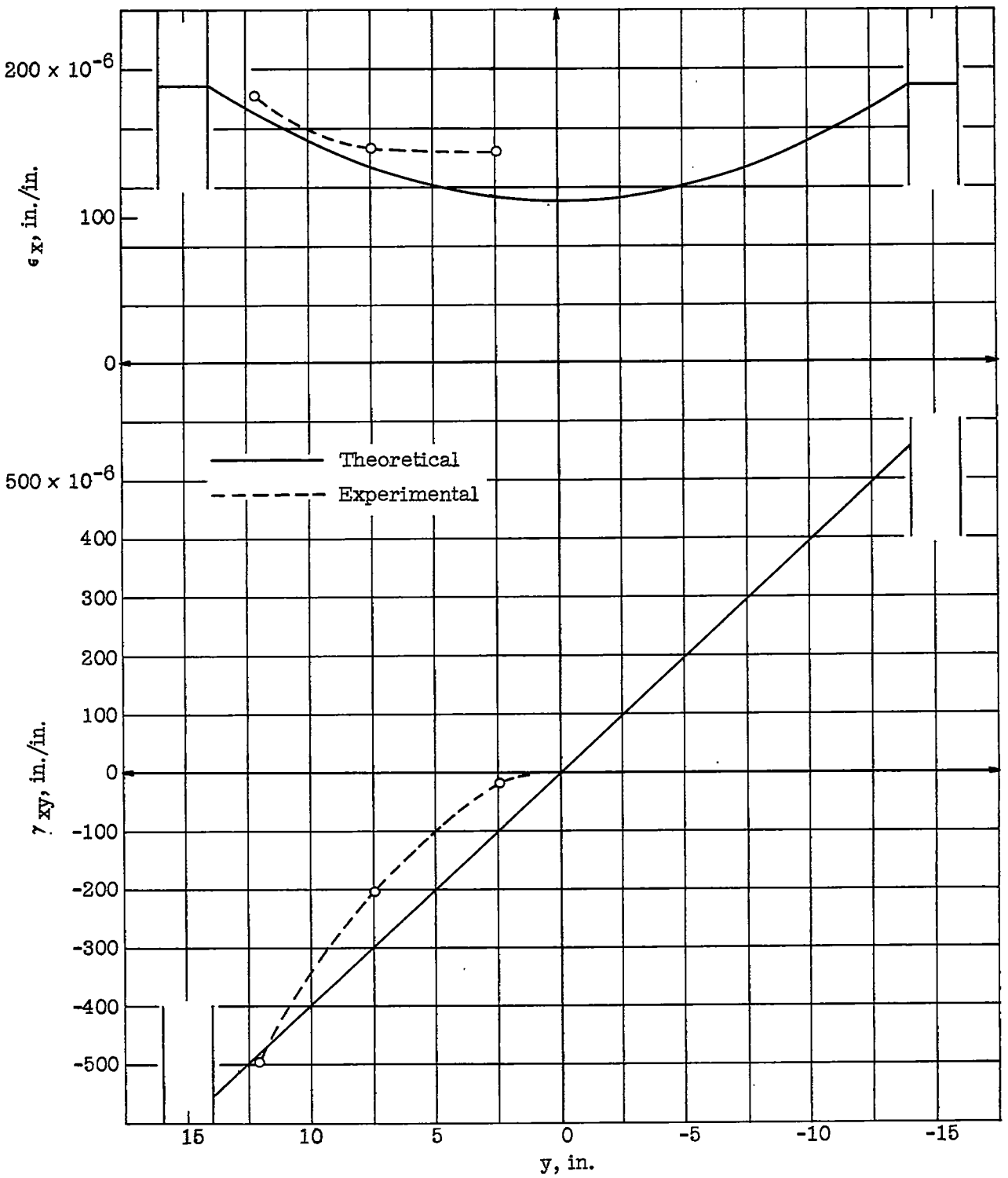

Figure 8.- Comparison of theoretical and experimental strains. Section 1. x = 22 inches.

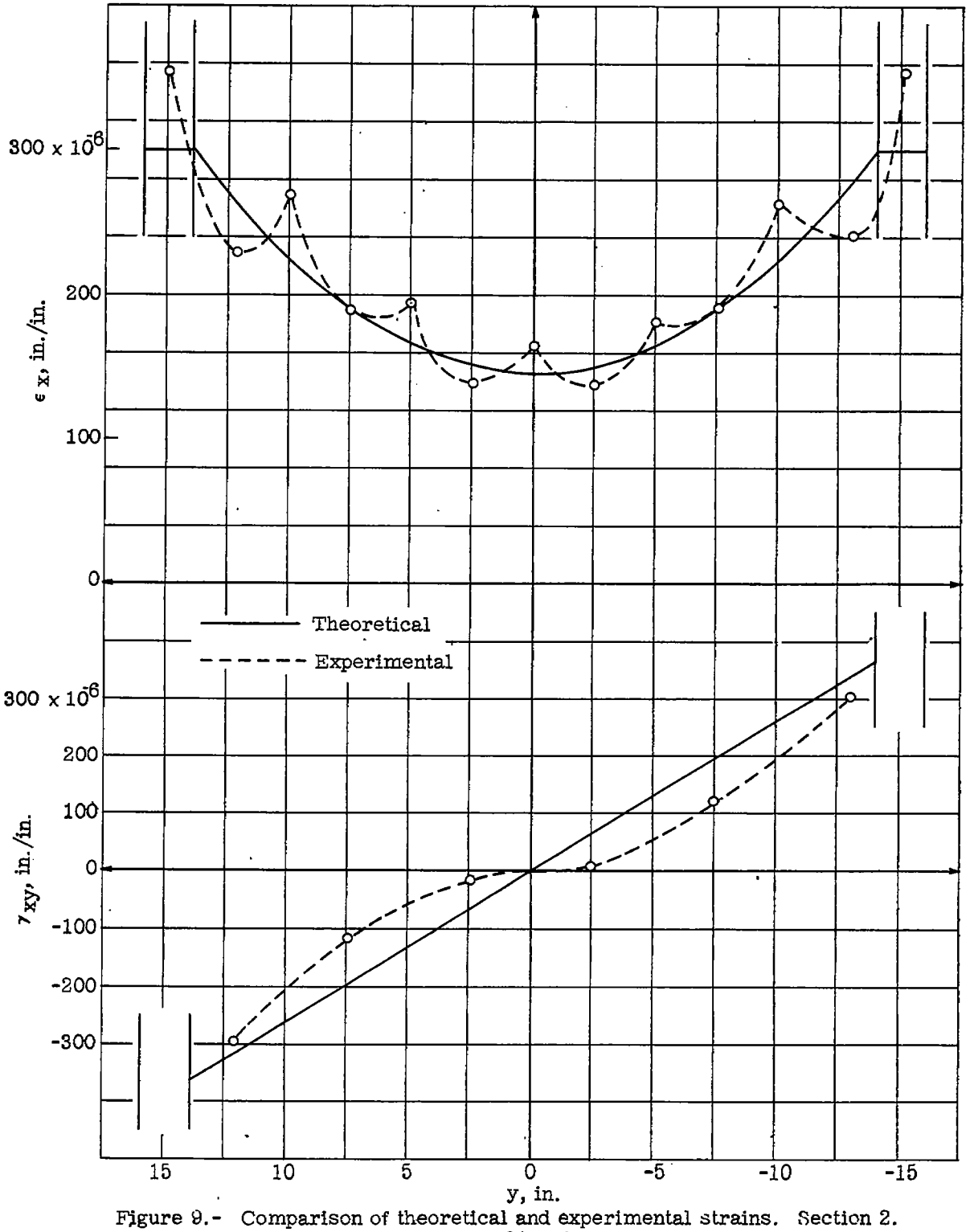

Figure 9.- Comparison of theoretical and experimental strains. Section 2. x = 34 inches.

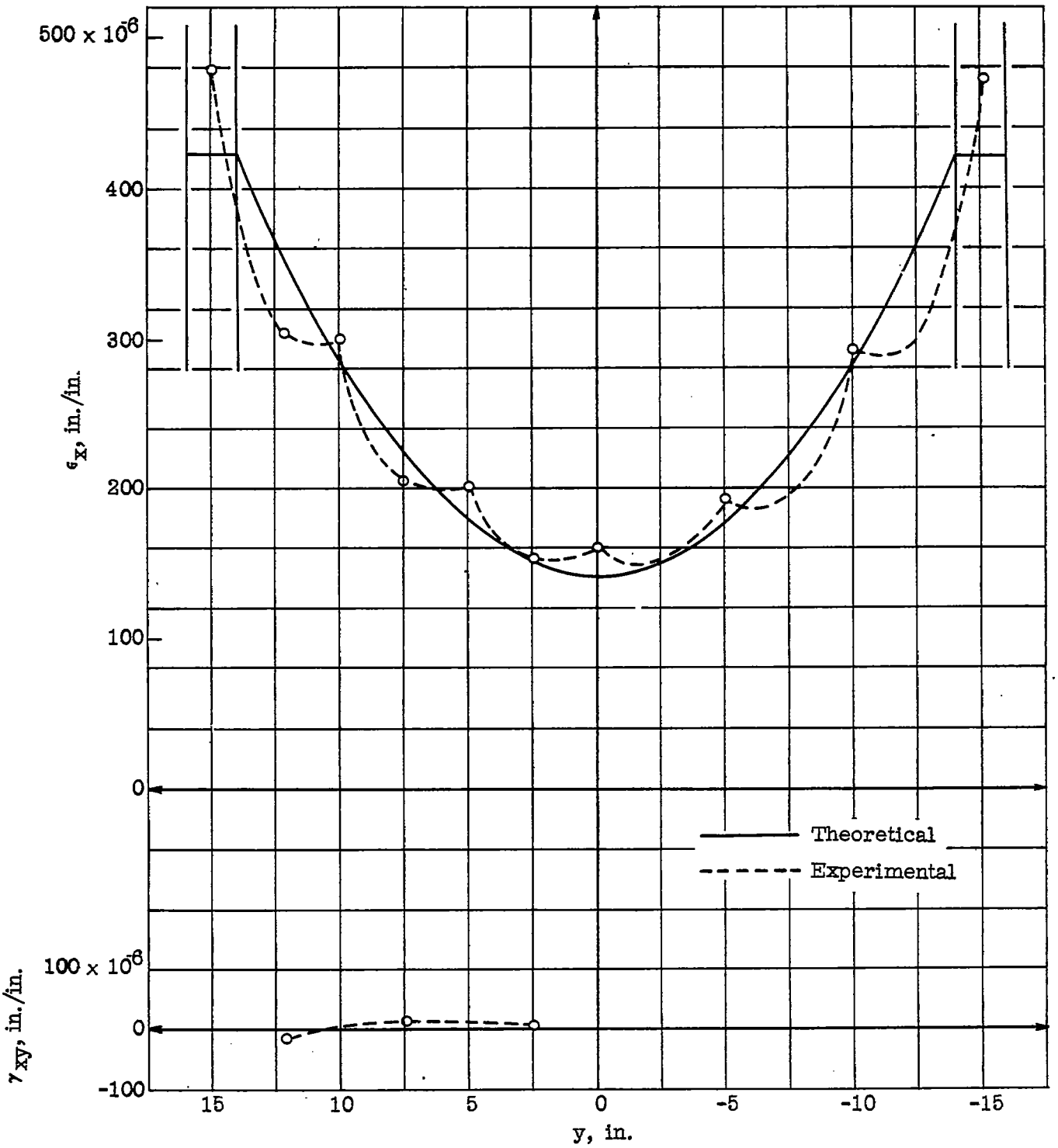

Figure 10.- Comparison of theoretical and experimental strains. Section 3. x = 46 inches.

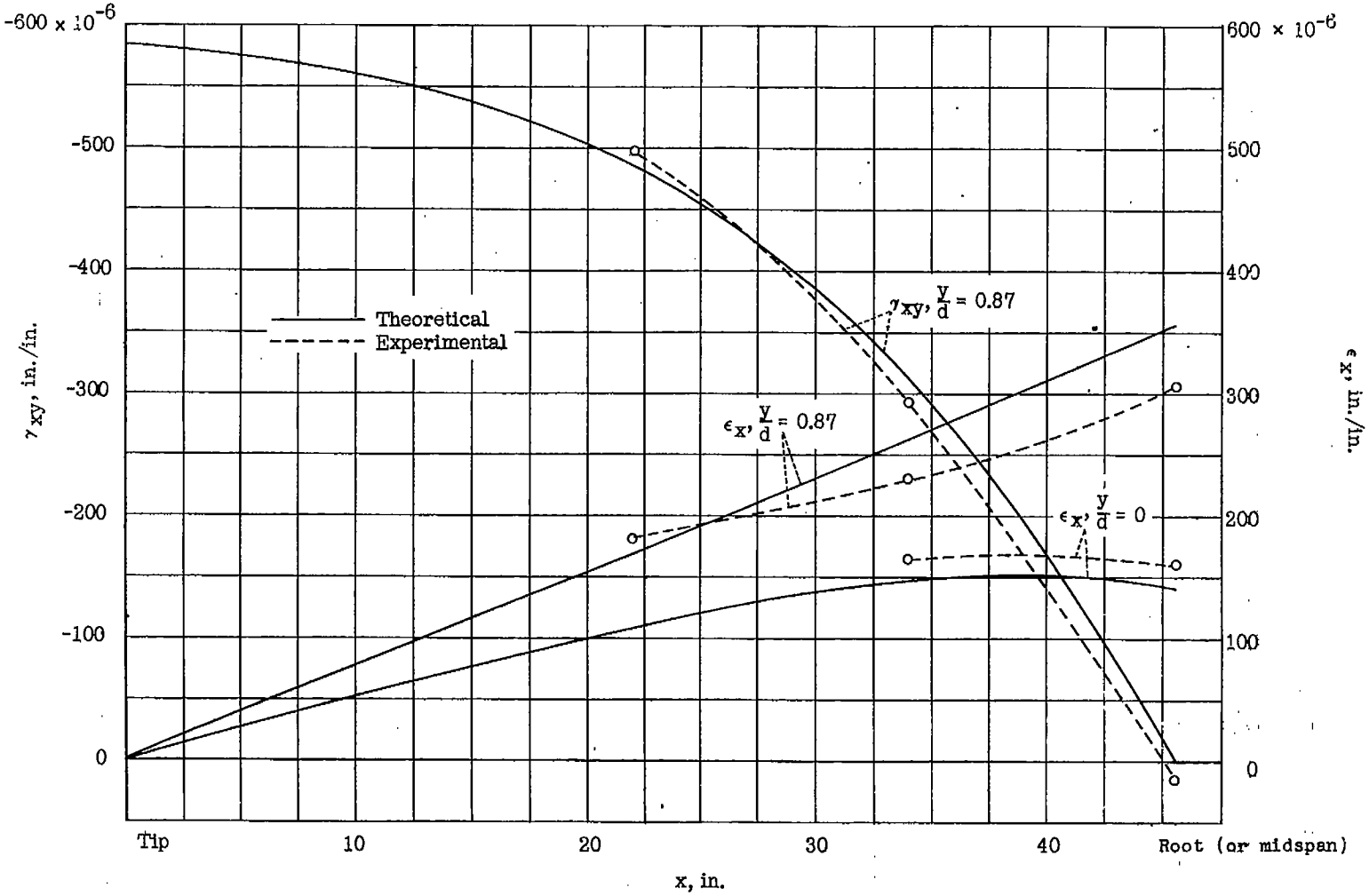

Figure 11.- Comparison of theoretical and experimental spanwise strain distributions.

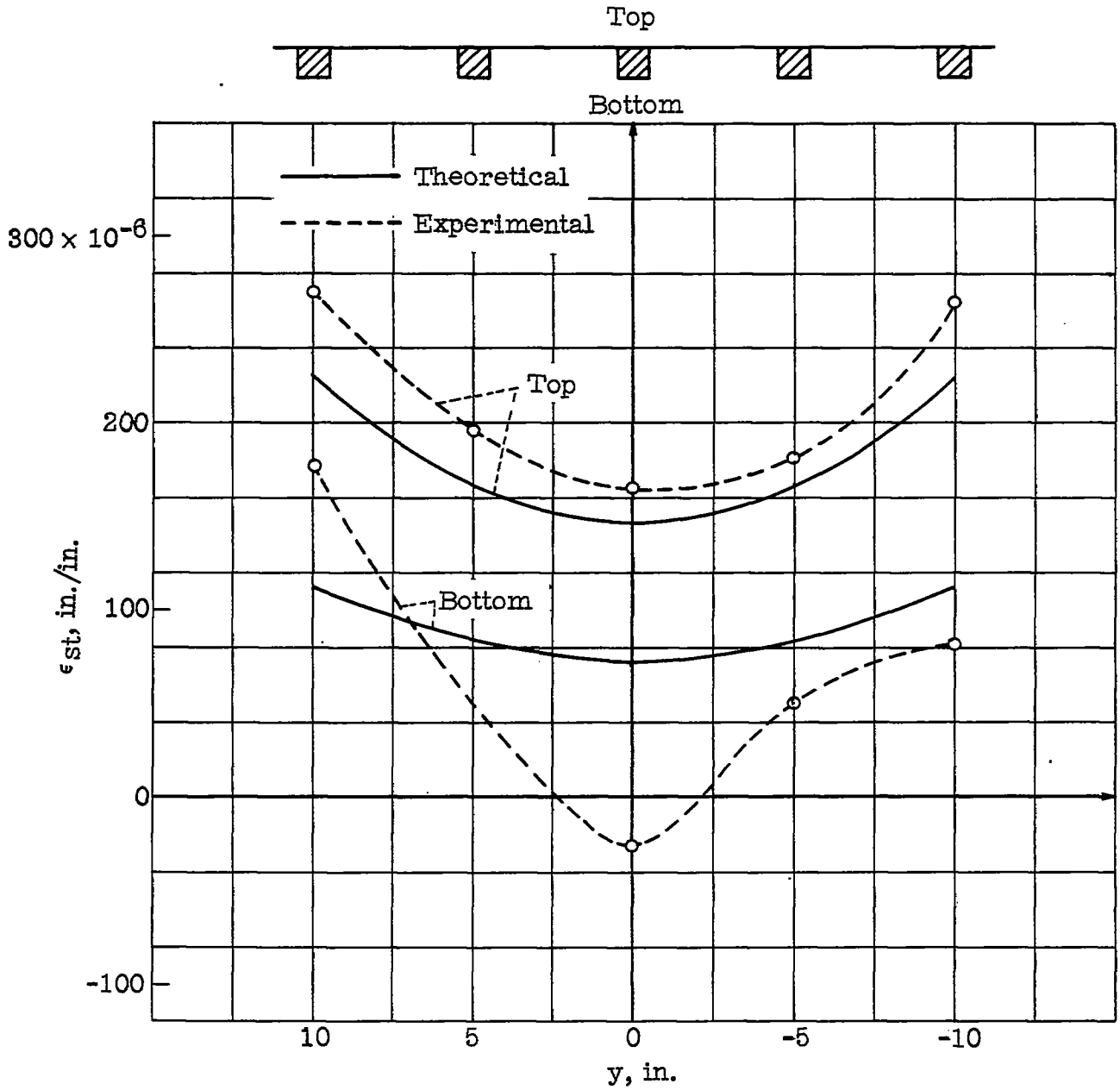

Figure 12.- Comparison of theoretical and experimental strains in stringers. Section 2. x = 34 inches.

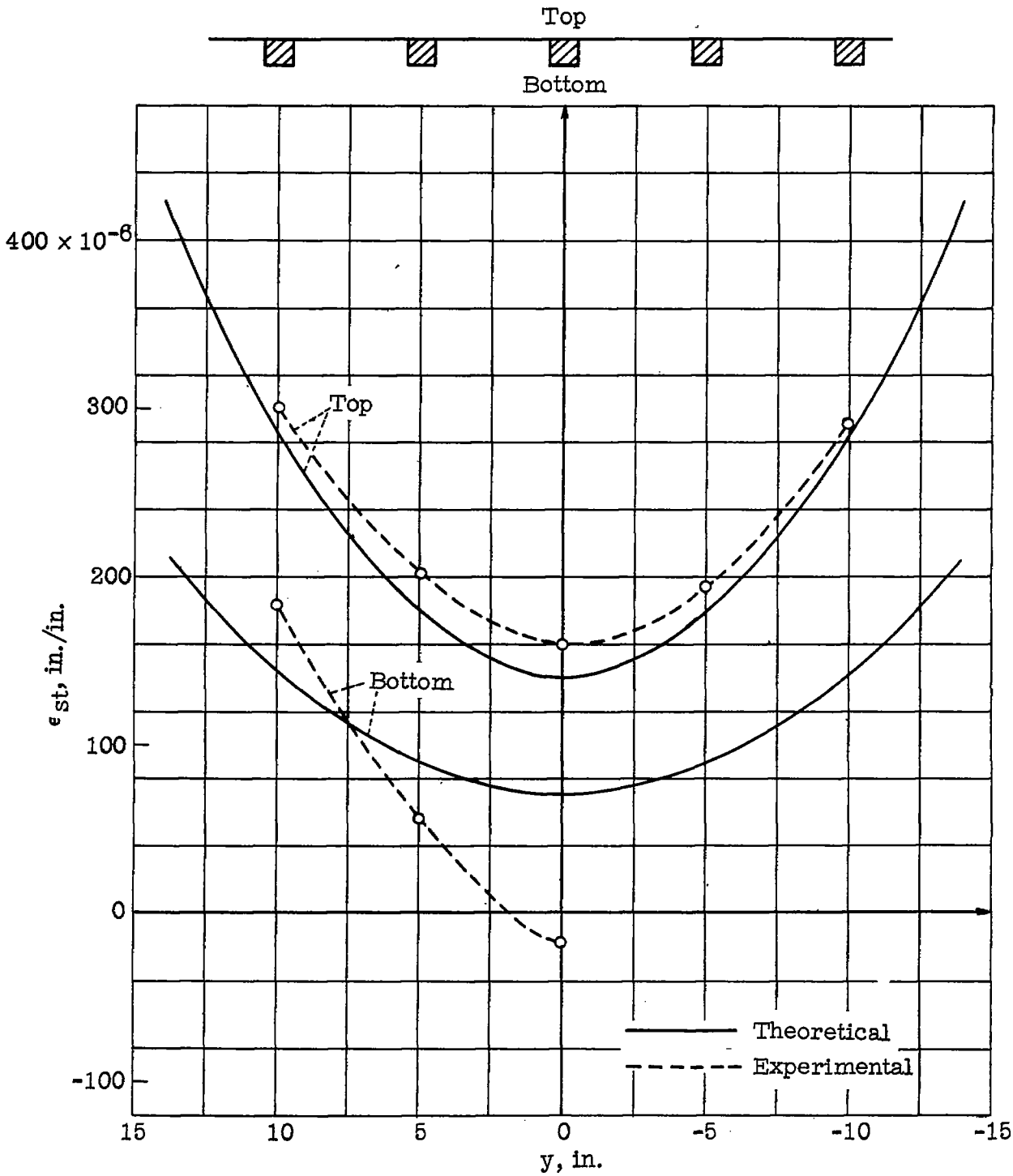

Figure 13.- Comparison of theoretical and experimental strains in stringers. Section 3. x = 46 inches.

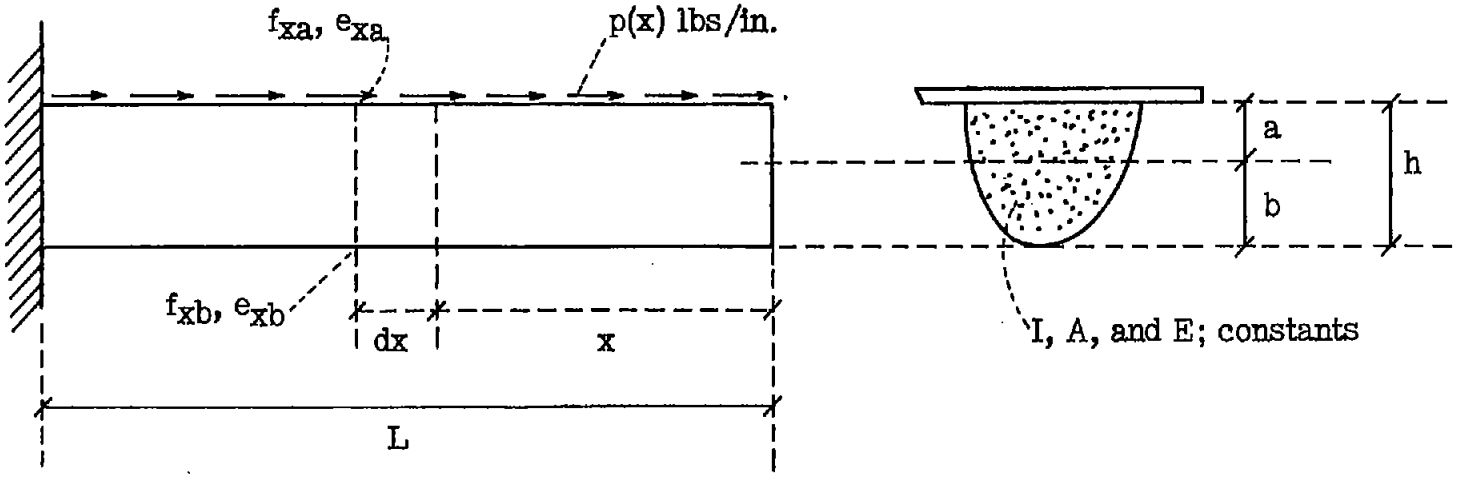

Figure 14.- Notation for simplified plate-stringer.

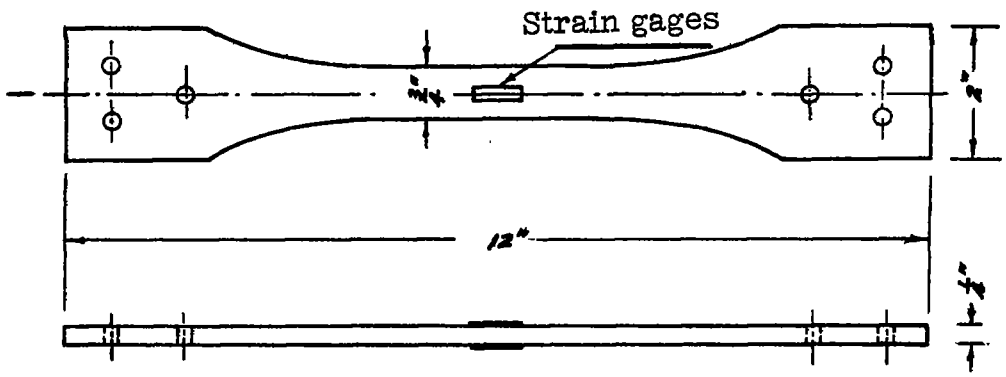

(a) Specimen for determination of E of longitudinal stringers.

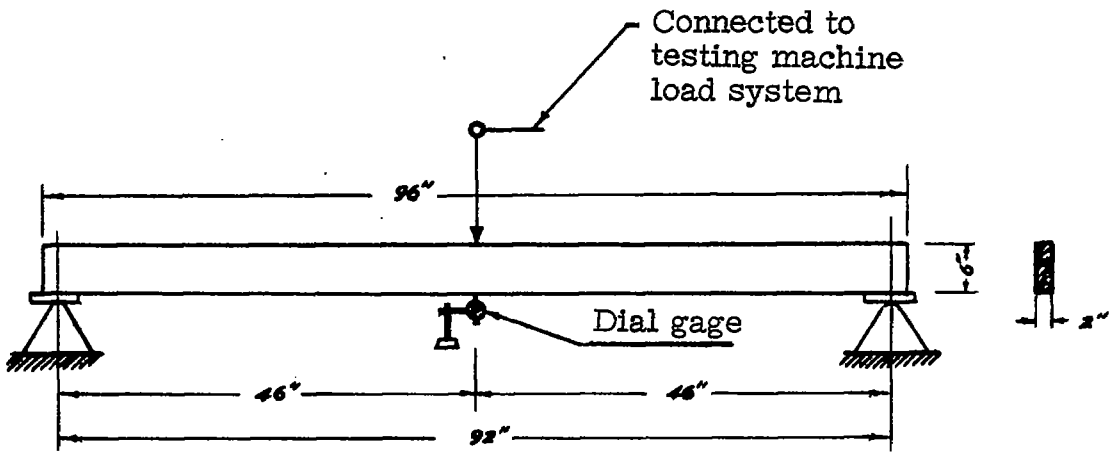

(b) Setup for determination of E of side members by bending.

Figure 15.- Property test for sugar pine members.

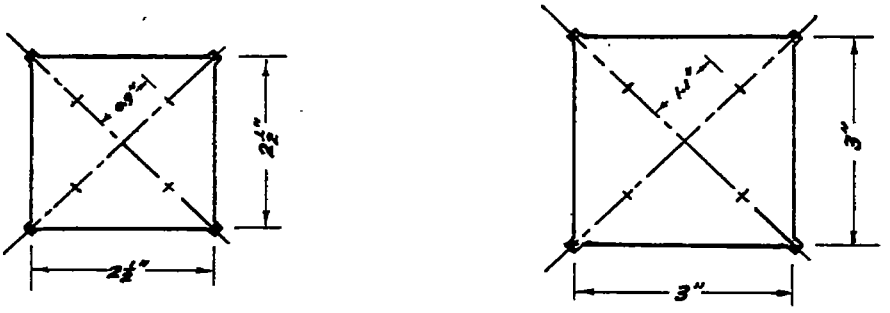

(a) Specimens for determination of G.

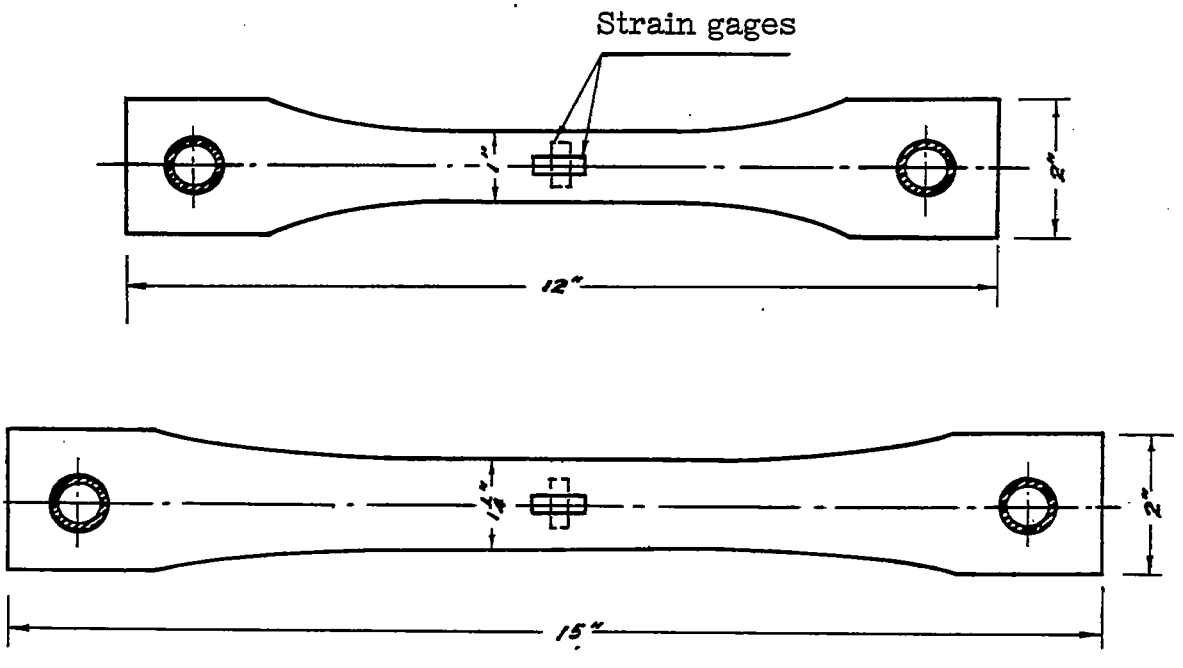

(b) Specimens for determination of E.

Figure 16.- Specimens for plywood property test.

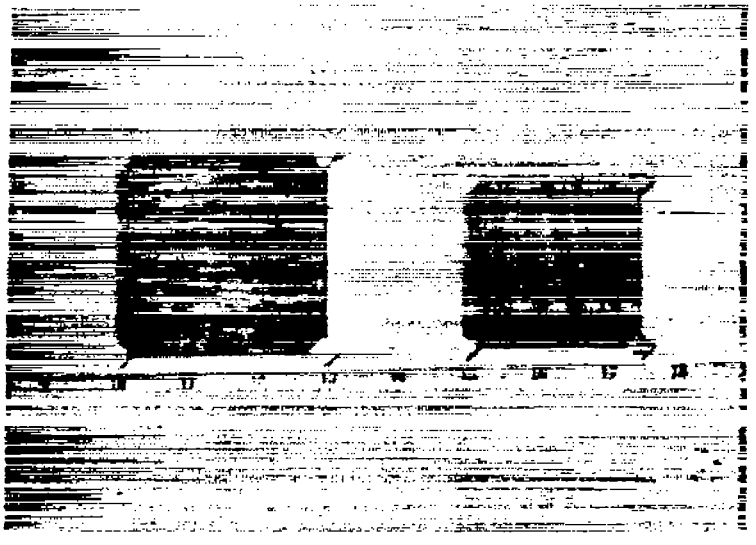

(a) Test specimens for determining G.

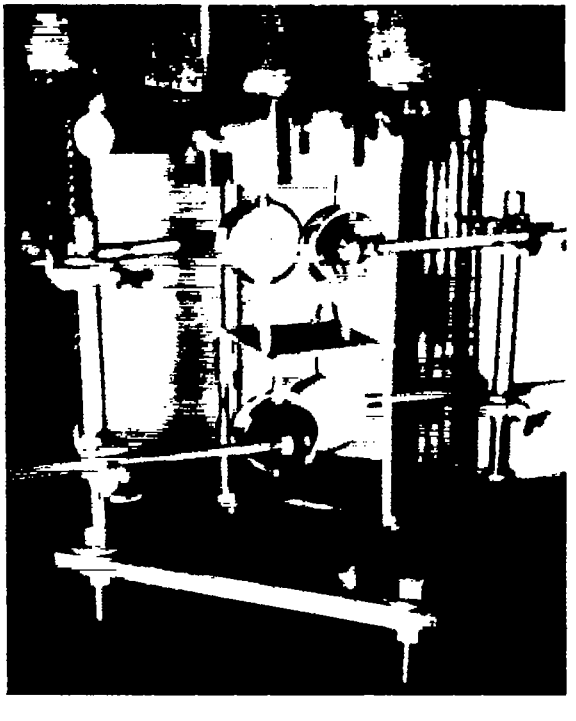

(b) Detail of loading device for determination of G.

Figure 17.- Test setup and specimens for determining shear modulus G.